New Type of Polymeric Indium Tellurides: Low-Temperature Synthesis and Structure Characterization of $[M(en)_3]In_2Te_6$ (M = Fe, Zn) and α- and β-$[Mo_3(en)_3(\mu_2\text{-}Te_2)_3(\mu_3\text{-}Te)(\mu_3\text{-}O)]In_2Te_6$

Jing Li,*,† Zhen Chen,† Thomas J. Emge,‡ and Davide M. Proserpio§

Department of Chemistry, Rutgers University, Camden, New Jersey 08102, Department of Chemistry, Rutgers University, Piscataway, New Jersey 08855, and Dipartimento di Chimica Strutturale e Stereochimica Inorganica, Università di Milano, 20133 Milano, Italy

Received June 24, 1996[⊗]

Crystal growth of metal tellurides and tellurometalates employing solvothermal reactions at temperatures below 200 °C have resulted in four new indium tellurium phases, $[Fe(en)_3](In_2Te_6)$ (**I**), $[Zn(en)_3](In_2Te_6)$ (**II**), and α- and β-$[Mo_3(en)_3(\mu_2\text{-}Te_2)_3(\mu_3\text{-}Te)(\mu_3\text{-}O)]In_2Te_6$ (**III-α** and **III-*β***). Single crystal X-ray diffraction analyses show that **I** and **II** are isostructural and belong to the orthorhombic crystal system, space group $P2_12_12_1$ (No. 19). Compound **I**: $a = 11.654$ (1) Å, $b = 12.968(2)$ Å, $c = 16.273(2)$ Å, $Z = 4$. Compound **II**: $a = 11.662(2)$ Å, $b = 12.948(2)$ Å, $c = 16.285(1)$ Å, $Z = 4$. The two polymorphs **III-α** and **III-*β*** crystallize in the monoclinic system. Compound **III-α**: $a = 11.815(2)$ Å, $b = 21.769(3)$Å, $c = 14.498(4)$ Å, $\beta = 95.43(2)°$, $Z = 4$, space group $P2_1/c$ (No. 14). Compound **III-*β***: $a = 22.154(3)$ Å, $b = 11.550(2)$Å, $c = 14.230(2)$ Å, $\beta = 99.05(1)°$, $Z = 4$, space group $P2_1/a$ (No. 14). All four are Zintl compounds containing novel one-dimensional polymeric chains of $^1_\infty[(In_2Te_6)^{2-}]$ that can be described as alternating fused five-membered rings $[(In^{3+})_2(Te_2^{2-})(Te^{2-})]$, joined at the In atoms.

Introduction

Solid state indium chalcogenides have been studied quite extensively. Many binary and ternary compounds have been synthesized and characterized. A variety of structures have been found which range from molecular (0-D) to chainlike (1-D), layered (2-D), and three-dimensional (3-D) extended systems. Examples of one-dimensional indium−chalcogen chains include edge sharing tetrahedra $^1_\infty[(In_2Q_4)^{2-}]$ ("Zweier" single chain)[1] in $AInQ_2$ (Q = Te and A = Na,[2a] K,[2a,b] Tl;[2c] Q = Se and A = Tl[2c]), in $A'In_2Te_4$ (A′ = Ca,[3] Ba,[2a] Sr[2a]), and in $[(C_4H_9)_4N]_2$-In_2Te_4.[4] More complex 1-D structures were observed in $Rb_4In_2Q_5$ (Q = S,[5a] Se[5b]) containing $^1_\infty[(In_2Q_5)^{4-}]$ formed by dimers of edge sharing tetrahedra $(In_2Q_6)^{6-}$ sharing one corner ("Vierer" single chain); in $Na_5In_2Te_6$,[6] containing $^1_\infty[(In_4Te_{12})^{10-}]$ Zweier single chains of corner sharing tetrahedra where two neighboring chains are joined further to form ribbons through ditelluro bridges; and in $Na_7In_3Se_8$,[7] containing $^1_\infty[(In_3Se_8)^{7-}]$, formed by alternating dimers of edge sharing tetrahedra and single tetrahedra ("Sechser" single chain).

Many of these compounds have been prepared at high temperatures via direct or chemical vapor transport reactions of elements and/or binary chalcogenides.[2a,c, 3,5−7] Some have also been synthesized by flux growth technique.[2b] The only low-temperature studies we have found so far (considering all indium chalcogenide compounds) are the crystal growth of the 1-D $[(C_4H_9)_4N]_2In_2Te_4$ by employing the electrochemical method at room temperature[4] and the synthesis of the Zintl compound $[(C_2H_5)_4N]_5In_3Te_7$ in liquid ammonia.[8]

Our recent explorations of low-temperature routes for the synthesis of solid state chalcogenides have focused mainly on solvothermal reactions, in which an organic (e.g., methanol) or an inorganic (e.g., water) solvent is used at temperatures below 200 °C. By incorporating chalcophilic elements into the reactions, we have successfully produced a number of new tellurides with extended one- or two-dimensional structural frameworks and molecular tellurometalates containing metals such as mercury,[9−12] tin,[13] gallium,[14] and antimony.[14] Most of these are not obtainable by high-temperature methods. In this article, we describe the solvothermal synthesis and structure characterization of a new group of indium 1-D chain compounds, $[Fe(en)_3](In_2Te_6)$ (**I**), $[Zn(en)_3](In_2Te_6)$ (**II**), and α- and β-$[Mo_3(en)_3(\mu_2\text{-}Te_2)_3(\mu_3\text{-}Te)(\mu_3\text{-}O)]In_2Te_6$ (**III-α** and **III-*β***).

† Rutgers University, Camden.
‡ Rutgers University, New Brunswick.
§ University of Milan.
⊗ Abstract published in *Advance ACS Abstracts,* February 15, 1997.

(1) We have adopted the crystal chemical classification used for silicate and for other tetrahedral compounds: the periodicity of a single chain is defined as the number of polyhedra within one repeating unit of the linear part of the chain. To denote a silicate anion according to its periodicity, the terms einer, zweier, dreier, etc., for periodicities 1, 2, 3, ..., have been widely accepted. These terms are derived from the German numerals, eins, zwei, drei, etc., by suffixing "er" to the numeral. See: Liebau, F. *Structural Chemistry of Silicates;* Springer: Berlin, 1985.
(2) (a) Franke, E. R.; Schäfer, H. *Z. Naturforsch.* **1972**, *37B*, 1308. (b) Hung, Y.-C.; Hwu, S.-J. *Acta Crystallogr.* **1993**, *C49*, 1588. (c) Müller, D.; Eulenberger, G.; Hahn, H. *Z. Anorg. Allg. Chem.* **1973**, *398*, 207.
(3) Klee, W.; Schäfer, H. *Z. Anorg. Allg. Chem.* **1981**, *479*, 125.
(4) Warren, C. J.; Haushalter, R. C.; Bocarsly, A. B. *J. Alloys Compd.* **1995**, *229*, 175.
(5) (a) Deiseroth, H. J. *Z. Naturforsch.* **1980**, *35B*, 953. (b) Krebs, B. *Angew. Chem., Int. Ed. Engl.* **1983**, *22*, 113.
(6) Eisenmann, B.; Hofmann, A.; Zagler, R. *Z. Naturforsch.* **1990**, *45B*, 8.
(7) Eisenmann, B.; Hofmann, A. *Z. Kristallogr.* **1991**, *197*, 159.
(8) Park, C.-W.; Salm, R. J.; Ibers, J. A. *Angew. Chem., Int. Ed. Engl.* **1995**, *34*, 1879.
(9) Li, J.; Rafferty, B. G.; Mulley, S.; Proserpio, D. M. *Inorg. Chem.* **1995**, *34*, 6417.
(10) Li, J.; Chen, Z.; Lam, K.-C.; Mulley, S.; Proserpio, D. M. *Inorg. Chem.,* in press.
(11) Li, J.; Chen, Z.; Proserpio, D. M. Manuscript in preparation.
(12) Li, J.; Chen, Z.; Kelley, J. L.; Mulley, S.; Proserpio, D. M. Manuscript in preparation.
(13) Li, J.; Chen. Z.; Proserpio, D. M.; Emge, T. J.; Tan, Y. Manuscript in preparation.
(14) Li, J.; Chen, Z.; Proserpio, D. M. Manuscript in preparation.

S0020-1669(96)00751-3 CCC: $14.00

Table 1. Crystallographic Data for **I**, **II**, **III-α**, and **III-*β***

	I	**II**	**III-α**	**III-*β***
chem formula	$[Fe(en)_3]In_2Te_6$	$[Zn(en)_3]In_2Te_6$	$[Mo_3(en)_3(\mu_2\text{-}Te_2)_3(\mu_3\text{-}Te)(\mu_3\text{-}O)]In_2Te_6$	
fw	1231.40	1240.92	2372.57	2372.57
space group	$P2_12_12_1$ (No. 19)	$P2_12_12_1$ (No. 19)	$P2_1/c$ (No. 14)	$P2_1/a$ (No. 14)
a, Å	11.654(1)	11.662(2)	11.815(2)	22.154(3)
b, Å	12.968(2)	12.948(2)	21.769(3)	11.550(2)
c, Å	16.273(2)	16.285(1)	14.498(4)	14.230(2)
β, deg			95.43(2)	99.05 (1)
V, Å^3	2459.3(5)	2459.0(6)	3712.2(13)	3595.8(9)
Z		4	4	4
ρ_{calc}, g cm^{-3}	3.326 g	3.352	4.245	4.383
μ, mm^{-1}	9.419	9.806	12.24	12.63
R^a [$I > 2\sigma(I)$]	R1, 0.035; $R2_w$[b], 0.071	R1, 0.022; $R2_w$[c], 0.047	R1, 0.048; $R2_w$[d], 0.090	R1, 0.072; $R2_w$[e], 0.150

[a] $R1 = \sum||F_o| - |F_c||/\sum|F_o|$. $R2_w = [\sum w(F_o^2 - F_c^2)^2/\sum wF_o^4]^{1/2}$. [b] Weighting: $w = 1/[\sigma^2(F_o^2) + (0.03P)^2 + 8.00P]$, where $P = (F_o^2 + 2F_c^2)/3$. [c] $w = 1/[\sigma^2(F_o^2) + (0.016P)^2 + 7.313P]$. [d] $w = 1/[\sigma^2(F_o^2) + (0.030P)^2 + 70.0P]$. [e] $w = 1/[\sigma^2(F_o^2) + (0.075P)^2 + 15.0P]$.

Experimental Section

Chemicals. Molybdenum(V) chloride, (98%, Aldrich Chemical Co.), Iron(II) chloride (99.5%, AESAR/Johnson Matthey), zinc chloride (98%, Fisher Scientific), indium(III) chloride (99.5%, Fisher), Te (99.8%, Aldrich), and binary alkali-metal precursors (A_2Te, A = Li, K, Rb, Cs) were used as starting materials. A_2Te were prepared by direct combination of stoichiometric amounts of alkali metal and Te in liquid ammonia. Ethylenediamine (99%, anhydrous, Fisher) was the solvent used in all reactions.

Crystal Growth of $[Fe(en)_3](In_2Te_6)$ (I). Single crystals of **I** were originally isolated in a ca. 30% yield from a solvothermal reaction containing 0.036 g (0.25 mmol) of Li_2Te, 0.052 g (0.25 mmol) of K_2-Te, 0.032 g (0.25 mmol) of $FeCl_2$, 0.050 g (0.25 mmol) of $InCl_3$, and 0.096 g (0.75 mmol) of Te as starting materials. These starting materials were weighed and mixed in a glovebox under inert argon atmosphere. A thick-wall Pyrex tube (9 mm o.d., ca. 5 in. long) was used as the reaction container. Approximately 5.5 mmol of the solvent, ethylenediamine (en), was added to the mixture. The tube was then sealed under vacuum ($\sim 10^{-3}$ Torr) after the liquid was condensed by liquid nitrogen. The sample was placed in an oven at 180 °C and was kept at this temperature for 7 days. After cooling to room temperature, the reaction product was washed with 35 and 95% ethanol and dried with diethyl ether. Black, rectangular blocklike crystals of **I** were found. The same crystals were also obtained using Li_2Te (1.0 mmol), $FeCl_2$ (0.25 mmol), $InCl_3$ (0.5 mmol), and Te (0.5 mmol) as reactants. Microprobe analysis was performed on the selected crystals using a JEOL JXA-8600 Superprobe. The results clearly indicated the presence of Fe, In, and Te in an approximate ratio of 1:2.3:6.6. A powder X-ray diffraction study of the sample also indicated the existence of $FeTe_2$.

Crystal Growth of $[Zn(en)_3](In_2Te_6)$ (II). Dark, platelike crystals of **II** were obtained by reactions of 0.099 g (0.25 mmol) of Cs_2Te, 0.034 g (0.25 mmol) of $ZnCl_2$, 0.050 g (0.25 mmol) of $InCl_3$, and 0.096 g (0.75 mmol) of Te. The sample was prepared in the same way as that described above for $[Fe(en)_3](In_2Te_6)$. The same heating and isolation scheme was also used. The approximate composition of **II** was obtained with the microprobe of a Kevex EDAX (energy dispersive analysis by X-ray) on a Hitachi S-2400 scanning electron microscope. Powder X-ray diffraction analysis on the final product indicated a ca. 35% yield of **II** with the rest of the sample being Te.

Crystal Growth of α- and *β*-$[Mo_3(en)_3(\mu_2\text{-}Te_2)_3(\mu_3\text{-}Te)(\mu_3\text{-}O)]$-$In_2Te_6$ (III-α, III-*β*). Crystals of **III-α**, **III-*β*** were also grown at 180 °C from a solvothermal reaction with the following initial composition of the reactants: 0.036 g (0.25 mmol) of Li_2Te, 0.052 g (0.25 mmol) of K_2Te, 0.033 g (0.25 mmol) of $MoCl_5$, 0.050 g (0.25 mmol) of $InCl_3$, and 0.096 g (0.75 mmol) of Te. The experimental conditions were identical to those given for **I** and **II**. Crystals of **III-α** were black columnar, while crystals of **III-*β*** were black elongated thin plates. A different reaction containing 1.25 mmol of Li_2Te, 0.75 mmol of $MoCl_5$, 0.5 mmol of $InCl_3$, and 0.75 mmol of Te produced mostly crystals of binary indium telluride. A microprobe analysis on the JEOL JXA-8600 Superprobe system yielded the approximate composition of Mo, In, and Te for both compounds; no Cl was found.

Single Crystal Structure Determination. The room temperature single-crystal X-ray diffraction experiments for **I**, **II**, **III-α**, and **III-*β*** have employed an Enraf-Nonius CAD4 diffractometer equipped with graphite monochromatized Mo Kα radiation. Data were collected with the ω-scan method for all four compounds. A 1.0° scan interval was used for **I**, and **III-α** and **-*β*** and a 0.9° for **II**. The 2θ limits were set at $4° < 2\theta < 50°$ for **I** and **III-α**, $6° < 2\theta < 50°$ for **II**, and $4° < 2\theta < 40°$ for **III-*β***. Data collection parameters, refinement results, and related data for all compounds are given in Table 1. All diffraction data were corrected for Lorentz and polarization effects, and for absorption, the latter using the numerical grid method in SHELX76 for **I**, and **III-α** and **-*β***, and an empirical absorption correction based on ψ-scans was applied for **II**. The crystal structures were solved by use of Patterson methods (SHELXS86)[15] and refined by use of full-matrix least-squares methods on F_o^2 (SHELXL93).[16] Crystal drawings were produced with SCHAKAL.[17] For $(In_2Te_6)^{2-}$ in both **III-α** and **-*β***, one Te atom of one of the ditelluride ligands was disordered, such that a second, minor site indicated another "puckering" conformation for the In_2Te_3 ring, but with only a site occupancy of 0.060(2) and 0.103(8), respectively, for the anions in **III-α** and **-*β***. This minor degree of disorder is thus modeled as two distinct sites for one Te (Te1A⋯Te1B > 0.6 Å) and as slightly elongated anisotropic displacement parameters for most of the other Te atoms in the anion. The mean square displacement for the anion Te atoms are more anisotropic in **III-*β*** than in **III-α** but not to the extent where any other Te site could be split (e.g., any possibly split site would have $D < 0.6$ Å). This situation is consistent with the expectation that minor differences in

Table 2. Significant Atomic Coordinates and Equivalent Isotropic Displacement Parameters (Å^2) for $[Fe(en)_3]In_2Te_6$ (**I**) (Top) and $[Zn(en)_3]In_2Te_6$ (**II**) (Bottom)[a]

atom	*x*	*y*	*z*	*U*(eq)
In1	0.7891(1)	0.4786(1)	0.3168(1)	0.033(1)
In2	0.7802(1)	0.5202(1)	0.0714(1)	0.036(1)
Te1	0.9823(1)	0.4057(1)	0.2319(1)	0.051(1)
Te2	0.9832(1)	0.5898(1)	0.1477(1)	0.057(1)
Te3	0.8383(1)	0.3329(1)	−0.0017(1)	0.046(1)
Te4	0.6630(1)	0.3288(1)	−0.1151(1)	0.049(1)
Te5	0.6217(1)	0.4857(1)	0.1951(1)	0.035(1)
Te6	0.7380(1)	0.6589(1)	−0.0538(1)	0.044(1)
In1	0.78811(6)	0.47828(5)	0.3166.8(4)	0.0320(2)
In2	0.77964(6)	0.52064(6)	0.0714.5(4)	0.0352(2)
Te1	0.98154(6)	0.40515(7)	0.23167(4)	0.0494(2)
Te2	0.98252(6)	0.59055(7)	0.14818(4)	0.0544(2)
Te3	0.83808(6)	0.33255(6)	−0.00104(5)	0.0454(2)
Te4	0.66370(7)	0.32852(6)	-0.11527(5)	0.0488(2)
Te5	0.62079(5)	0.48615(5)	0.19489(4)	0.0344(2)
Te6	0.73860(7)	0.65949(5)	-0.05397(4)	0.0434(2)

[a] *U*(eq) is defined as one-third of the trace of the orthogonalized U_{ij} tensor.

(15) Sheldrick, G. M. *Acta Crystallogr.* **1990**, *A46*, 467.
(16) Sheldrick, G. M. *SHELX-93*: *Program for structure refinement*; University of Goettingen: Goettingen, Germany, 1994.
(17) Keller, E. *SCHAKAL 92*: *A computer program for the graphical representation of crystallographic models*; University of Freiburg: Freiburg, Germany, 1992.

Table 3. Significant Atomic Coordinates and Equivalent Isotropic Displacement Parameters (Å^2) for α-[$Mo_3(en)_3(\mu_2\text{-}Te_2)_3(\mu_3\text{-}Te)(\mu_3\text{-}O)$]$In_2Te_6$ (**III-α**) (Top) and for *β*-[$Mo_3(en)_3(\mu_2\text{-}Te_2)_3(\mu_3\text{-}Te)(\mu_3\text{-}O)$]$In_2Te_6$ (**III-*β***) (Bottom)[a]

atom	*x*	*y*	*z*	*U*(eq)
Mo1	0.7136(1)	0.5714(1)	0.3690(1)	0.023(1)
Mo2	0.5967(1)	0.6569(1)	0.2600(1)	0.023(1)
Mo3	0.7127(1)	0.5651(1)	0.1814(1)	0.019(1)
Te1	0.3804(1)	0.4793(1)	0.2589(1)	0.040(1)
Te2	0.4794(1)	0.5766(1)	0.1376(1)	0.030(1)
Te3	0.6248(1)	0.6624(1)	0.0681(1)	0.034(1)
Te4	0.6323(1)	0.4657(1)	0.2769(1)	0.029(1)
Te5	0.8698(1)	0.4939(1)	0.2918(1)	0.031(1)
Te6	0.4811(1)	0.5850(1)	0.3784(1)	0.033(1)
Te7	0.6284(1)	0.6770(1)	0.4535(1)	0.039(1)
O1	0.7638(9)	0.6313(5)	0.2742(8)	0.043(3)
N1	0.8723(11)	0.6032(7)	0.4546(9)	0.038(3)
N2	0.7244(11)	0.5130(7)	0.5013(9)	0.038(3)
N3	0.4469(10)	0.7215(6)	0.2457(9)	0.031(3)
N4	0.6749(11)	0.7518(6)	0.2574(11)	0.041(4)
N5	0.8712(10)	0.5903(5)	0.1191(9)	0.028(3)
N6	0.7175(10)	0.5017(6)	0.0576(9)	0.031(3)
In1	−0.1501(1)	0.2893(1)	−0.0258(1)	0.034(1)
In2	−0.1223(1)	0.3093(1)	0.2399(1)	0.032(1)
Te8	0.0831(1)	0.2878(1)	0.0483(1)	0.035(1)
Te9	0.0743(1)	0.3698(1)	0.1913(1)	0.047(1)
Te1A	−0.0565(1)	0.1878(1)	0.2038(1)	0.038(1)
Te11	−0.1826(1)	0.1281(1)	0.3268(1)	0.037(1)
Te12	−0.2931(1)	0.3332(1)	0.0984(1)	0.032(1)
Te13	−0.1782(1)	0.3307(1)	0.4162(1)	0.040(1)
Mo1	0.0596(2)	0.1466(4)	0.2674(4)	0.026(1)
Mo2	0.1480(2)	0.2665(4)	0.3816(3)	0.026(1)
Mo3	0.0522(2)	0.3804(4)	0.2800(3)	0.024(1)
Te1	−0.0205(2)	0.2319(4)	0.5403(3)	0.043(1)
Te2	0.0727(2)	0.3995(4)	0.4774(3)	0.035(1)
Te3	0.1521(2)	0.5094(4)	0.3700(3)	0.040(1)
Te4	−0.0423(2)	0.2460(4)	0.3274(3)	0.034(1)
Te5	−0.0267(2)	0.2656(4)	0.1353(2)	0.036(1)
Te6	0.0820(2)	0.0968(4)	0.4601(3)	0.035(1)
Te7	0.1671(2)	0.0311(4)	0.3454(3)	0.040(1)
O1	0.1173(13)	0.2759(27)	0.2395(23)	0.033(5)
N1	0.0839(18)	0.0737(35)	0.1339(27)	0.030(6)
N2	0.0052(17)	−0.0219(34)	0.2504(27)	0.031(6)
N3	0.2196(14)	0.2576(38)	0.5173(26)	0.030(7)
N4	0.2401(16)	0.2921(39)	0.3373(30)	0.039(7)
N5	0.0676(16)	0.4833(34)	0.1537(26)	0.025(6)
N6	−0.0121(16)	0.5335(30)	0.2781(27)	0.023(6)
In1	−0.2000(2)	−0.2524(5)	0.1669(3)	0.045(1)
In2	−0.2824(2)	−0.0009(4)	0.0227(3)	0.042(1)
Te8	−0.1533(2)	−0.0638(5)	0.2739(3)	0.070(2)
Te9	−0.1730(2)	0.0839(5)	0.1196(4)	0.076(2)
Te1A	−0.2533(2)	−0.0851(5)	−0.1490(3)	0.055(2)
Te11	−0.3233(2)	0.0532(5)	−0.2818(3)	0.056(1)
Te12	−0.3215(2)	−0.2019(4)	0.1030(3)	0.052(1)
Te13	−0.3557(2)	0.1949(4)	−0.0096(3)	0.047(1)

[a] *U*(eq) is defined as one-third of the trace of the orthogonalized $\mathbf{U}_{ij}$ tensor.

the puckering of the rings within the anion chains can exist in these crystal structures. All H atoms were placed in their calculated sp^3 geometry positions with C−H of 0.95Å and H−H of 0.90 Å. The following restraints were used in the structure refinement. For **III-α**, the U_{ij} components of all O, N, and C atoms were restrained with an effective standard deviation of 0.02 Å^2 to isotropic behavior, but the corresponding isotropic *U* was free to vary; these restraints added 0.19 to the $\langle w\delta^2 \rangle$ term minimized in the final cycle of least-squares refinement. For **III-*β***, (a) the U_{ij} components of all O, N, and C atoms were restrained with an effective standard deviation of 0.015 Å^2 to isotropic behavior, but the corresponding isotropic *U* was free to vary; (b) the U_{ij} components of the Mo, O, N, and C atoms in the direction of the Mo−N, N−C, C−C, or Mo−O bond were restrained to be equal within the effective standard deviation of 0.015 Å^2; and (c) the Mo−N, N−C, and C−C bonds were restrained to be equal to 2.3, 1.5, and 1.5 Å, with effective standard deviations of 0.10, 0.05, and 0.05 Å, respectively these restraints added 0.21, 0.16, and 0.53 to the $\langle w\delta^2 \rangle$ term minimized in the final cycle of least-squares refinement, respectively).

Table 4. Selected Bond Lengths (Å) for $[Fe(en)_3]In_2Te_6$ (**I**) and $[Zn(en)_3]In_2Te_6$ (**II**)

	I	II		I	II
In1−Te6	2.777(2)	2.7778(9)	In1−Te5	2.782(1)	2.7842(9)
In1−Te4	2.788(2)	2.7932(11)	In1−Te1	2.805(2)	2.8110(10)
In2−Te6	2.761(2)	2.7628(10)	In2−Te5	2.768(1)	2.7699(9)
In2−Te3	2.788(2)	2.7909(11)	In2−Te2	2.820(2)	2.8246(11)
Te1−Te2	2.753(2)	2.7589(13)	Te3−Te4	2.753(2)	2.7567(11)

Table 5. Selected Bond Lengths (Å) for α-[$Mo_3(en)_3(\mu_2\text{-}Te_2)_3(\mu_3\text{-}Te)(\mu_3\text{-}O)$]$In_2Te_6$ (**III-α**) and *β*-[$Mo_3(en)_3(\mu_2\text{-}Te_2)_3(\mu_3\text{-}Te)(\mu_3\text{-}O)$]$In_2Te_6$ (**III-*β***)

	III-α	III-*β*		III-α	III-*β*
In1−Te12	2.754(2)	2.764(6)	In1−Te8	2.861(2)	2.764(7)
In1−Te13	2.754(2)	2.788(5)	In1−Te11	2.792(2)	2.777(7)
In2−Te13	2.739(2)	2.780(6)	In2−Te12	2.785(6)	2.787(2)
In2−Te9	2.818(2)	2.771(6)	In2−Te1A	2.820(2)	2.797(6)
Te8−Te9	2.745(2)	2.761(8)	Te1A−Te11	2.755(2)	2.757(7)
3× Mo−Mo	2.728(6)	2.715(7)	3× Mo−O1	2.03(1)	2.04(3)
6× Mo−N	2.26(2)	2.26(4)	3× Te−Te	2.82(4)	2.80(2)
Mo−Te2,4,6	2.779(6)	2.778(6)	Mo−Te3,5,7	2.82(1)	2.810(7)
Te1−Te2,4,6	3.03(4)	3.06(6)			

The final atomic fractional coordinates and isotropic equivalent displacement parameters are given for the anions in the structures of **I** and **II** (Table 2) and for all the significant atoms of **III-α** and **III-*β*** (Table 3). Selected bond distances are given in Table 4 for **I** and **II** and in Table 5 for **III-α** and **-*β***.

Results and Discussion

Synthesis. The synthesis of the title compounds indicates a somewhat complex oxidation−reduction process involving Te and Te^{2-} species. In the case of the Fe complex, the oxidation states of both Fe and In remained unchanged during the crystal formation of **I**. A similar situation applies to the Zn complex, where neither Zn nor In were involved in the oxidation−reduction process leading to the final product **II**. However, both **I** and **II** contain $(Te_2)^{2-}$ species which most likely resulted from either an oxidation of Te^{2-} or a reduction of Te, provided as reactants. Although none of the alkali metals (Li, K, and Cs) used in the reactions became part of the products, A_2Te seemed necessary as the reducing agent required for the oxidation−reduction reaction to take place. A separate set of experiments was conducted for the Fe complex in which only one type of A_2Te was used in each reaction. The results indicated that Li_2-Te served better for the crystal growth of **I**. The formation of **III-α** and **-*β*** also involved reduction of the transition metals, in which molybdenum was reduced from Mo(V) to Mo(IV). The source of oxygen atoms found in these two structures may likely come from one of the starting materials, $MoCl_3$ (98%).

Crystal Structures. All four compounds possess a common structural feature; that is, they are all composed of a transition metal coordination complex as cation and a polymeric indium−tellurium Zintl anion.

The structure of **I** contains linear channels of $[Fe(en)_3]^{2+}$ cations adjacent to polymeric chains of $^1_\infty[(In_2Te_6)^{2-}]$ anions propagating along the crystallographic *c* axis. A view of a single chain of the anion is shown in Figure 1. The $[Fe(en)_3]^{2+}$ geometry and stereochemistry are as expected for en complexes (see, e.g., ref 9). The average Fe−N distance is 2.21(1) Å and is in agreement with high-spin Fe(II) amine complexes.[18] The one-dimensional chain of the $(In_2Te_6)^{2-}$ anion in **I** can

(18) Katz, B. A.; Strouse, C. E. *Inorg. Chem.* **1980**, *19*, 658. Katz, B. A.; Strouse, C. E. *J. Am. Chem. Soc.* **1979**, *101*, 6214.

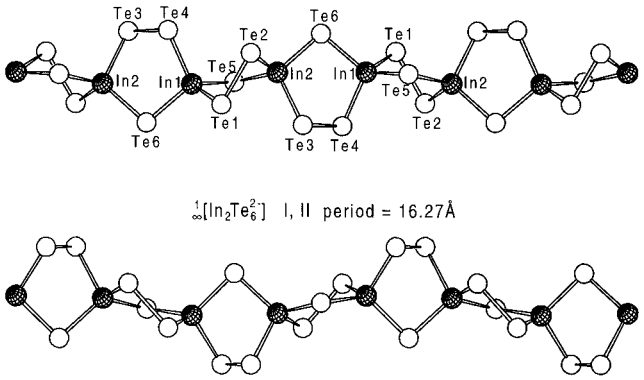

Figure 1. Two perpendicular views of the polymeric chain $^1_\infty(In_2Te_6)^{2-}]$ for **I** and **II**. The cross-hatched circles are In atoms and the open circles Te.

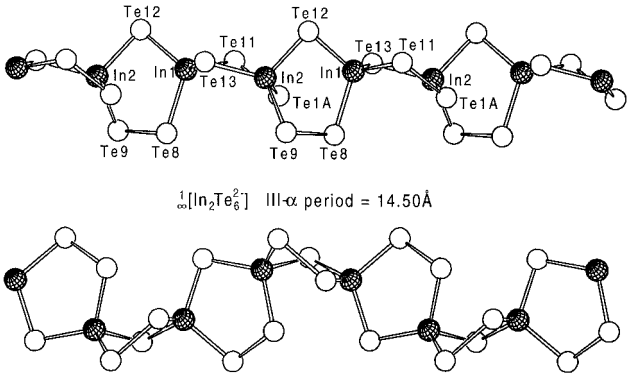

Figure 2. Two perpendicular views of the polymeric chain $^1_\infty[(In_2Te_6)^{2-}]$ for **III-α**. The cross-hatched circles are In atoms and the open circles Te.

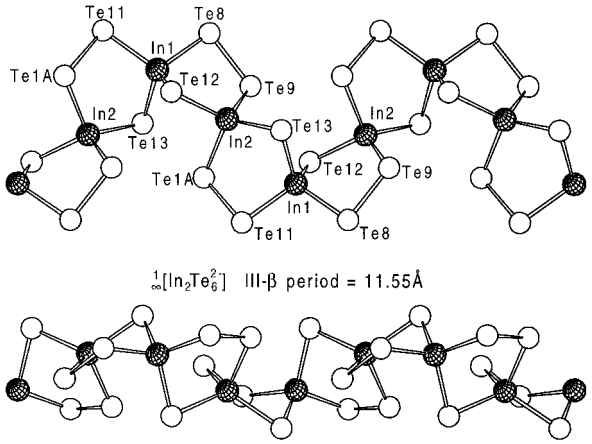

Figure 3. Two perpendicular views of the polymeric chain α$[(In_2Te_6)^{2-}]$ for **III-*β***. The cross-hatched circles are In atoms and the open circles Te.

be described as alternating fused five-membered rings $[(In^{3+})_2(Te_2^{2-})(Te^{2-})]$, joined at the In atoms (see Figure 1). The repeating unit consists of four In_2Te_3 rings with a period of 16.27 Å (equal to the unit cell *c* axis) resulting in a "Vierer" single chain. All In have a tetrahedral coordination with Te. The In−Te distances are comparable with other indium telluride compounds, such as those observed in the 1-D compounds listed above.[2−8] Compounds containing group 13/chalcogen five-membered rings include $InSe_4$ in the isolated anions $[In_2(Se_4)_2(Se_5)_2]^{4-}$, $[In_2Se_2(Se_4)_2]^{3-}$, and $[In_3Se_3(Se_4)_3]^{3-}$ [19a] and Tl_2Se_3, $TlSe_4$, and Tl_2Se_2 rings in $(Tl_4Se_{16})^{4-}$.[19b] However, as far as we are aware, such an $^1_\infty[(In_2Te_6)^{2-}]$ polymeric chain has not been reported previously, nor have any other indium tellurium compounds containing five-memberd rings. There are, however, several mercury tellurides containing one-dimensional chains formed by five-membered $(Hg_2Te_3)^{m-}$ rings. These are $^1_\infty[(Hg_2Te_9)^{4-}]$, $^1_\infty[(Hg_2Te_5)^{2-}]$, and $^1_\infty[(Hg_3Te_7)^{4-}]$ previously reported by us or by others.[19c,d]

For compound **II**, the molecular structure and crystal packing motif are essentially the same as those for **I**, since these two are isostructural. For the cation, the average Zn−N distance is 2.19(2) Å and is in agreement with the previously reported compounds with $[Zn(en)_3]^{2+}$.[20]

The crystal growth of $[Mo_3(en)_3(\mu_2\text{-}Te_2)_3(\mu_3\text{-}Te)(\mu_3\text{-}O)]In_2Te_6$ has yielded two polymorphs α and *β* that differ in their crystal packing motifs, mainly in the strikingly different puckering and disposition of the In_2Te_3 rings along the $^1_\infty[(In_2Te_6)^{2-}]$ chain. This is observed in the period of the chain of 14.50 and 11.55 Å, respectively, equal to the length of the unit cell axis *b* and *c* (see Figures 2 and 3). Although both of these compounds have monoclinic crystal symmetries (and primitive lattices), the unique *b* axis is along the $^1_\infty[(In_2Te_6)^{2-}]$ polymer direction for *β* but perpendicular to it in α (the anion polymer axis in **III-α** is along the *c* axis).

The anions for the three unique structures here, e.g., **I** and **III-α** and **-*β***, are all $(In_2Te_6)^{2-}$ polymeric chains of "fused" In_2Te_3 five-membered rings; however, the confines of the three unit cells are dramatically different, and the apparent high degree of flexibility of this anion is expressed in the different lengths of the repeated unit of four five-membered rings, the periods of this Vierer single chains are as follows: 16.27 Å for **I**, 16.28 Å for **II**, 14.50 Å for **III-α** and 11.55 Å for **III-*β***. The small variations in In−Te bond lengths observed for the three chains are summarized in Table 6 together with the averaged tetrahedral angles around the In. These variations do not account for the different stretchings of the repeated unit. Apparently, neither the In−Te nor Te−Te interactions determine the final stretching of the chains, so it must be some other secondary force that plays a role in the packing of the crystal. We have tried to characterize the differences in periods considering the In···In long contacts. One way is to imagine an ideal, nonstretched chain of In_2Te_3 pentagons with all of the In aligned and measure the stretching factor (*f*)[21] of the Vierer chain as the ratio between the observed period and the sum of the four In···In distances. The calculated *f* (see Table 6) correlates well with the observed period. Finally, the difference in the symmetry of the chains is evident when views along the chain for the three polymers (Figure 4) are compared. Compounds **I, II**, and **III-*β*** run parallel to a screw axis 2_1, while **III-α** lies on a glide plane.

The molecular structure of $[Mo_3(en)_3(\mu_2\text{-}Te_2)_3(\mu_3\text{-}Te)(\mu_3\text{-}O)]^{2+}$ has nearly C_{3v} symmetry and is shown in Figure 5 for the α polymorph (the cation for the *β* is very similar to the α one). This cation contains the $Mo_3L_3(\mu_2\text{-}Q_2)_3(\mu_3\text{-}Q')$ core found in several structures with nine-coordinate Mo(IV) atoms,[22] where L = terminal ligand (e.g., disulfide S_2^{2-} and diselenide Se_2^{2-}), Q = doubly bridging disulfide or diselenide, and Q′ = triply

(19) (a) Dhingra, S. S.; Kanatzidis, M. G. *Inorg. Chem.* **1995**, *32*, 1350. (b) Dhingra, S.; Liu, F.; Kanatzidis, M. G. *Inorg. Chim. Acta* **1993**, *210*, 237. (c) Haushalter, R. C. *Angew. Chem., Int. Engl.* **1985**, *24*, 433. Dhingra, S. S.; Warren, C. J.; Haushalter, R. C.; Bocarsly, A. B. *Chem. Mater.* **1994**, *6*, 2382. (d) Reference 9.

(20) See, e.g.: Cernak, J.; Chomic; Dunaj-Jurco, M.; Kappenstein, C. *Inorg. Chim. Acta* **1984**, *85*, 219. Emsley, J.; Arif, M.; Bates, P. A.; Hursthouse M. B. *Inorg. Chim. Acta* **1989**, *165*, 191.

(21) See: Ref. 1; p 80. Li, J.; Liszewski, Y. Y.; MacAdams, L. A.; Chen, F.; Mulley, S.; Proserpio, D. M. *Chem. Mater.* **1996**, *8*, 598.

(22) Liao, J.-H.; Li, J.; Kanatzidis, M. G. *Inorg. Chem.* **1995**, *34*, 2658, and references cited therein.

Table 6. Selected Averaged Bond Lengths (Å), Angles (deg), and Stretching Factors (*f*) (See Text) for the "Vierer" Single Chains $^1_\infty[(In_2Te_6)^{2-}]$

	4 × In−(Te_2)	4 × In−Te	Te−Te	6 × Te−In−Te	In···In	*f*	period (Å)
I, II	2.80(1)	2.77(1)	2.75(1)	109(6)	4.03/4.22	0.98	16.27
III-α	2.82(3)	2.76(2)	2.75(1)	109(6)	4.06/3.86	0.91	14.50
III-*β*	2.78(1)	2.78(1)	2.75(1)	109(7)	3.85/3.92	0.74	11.55

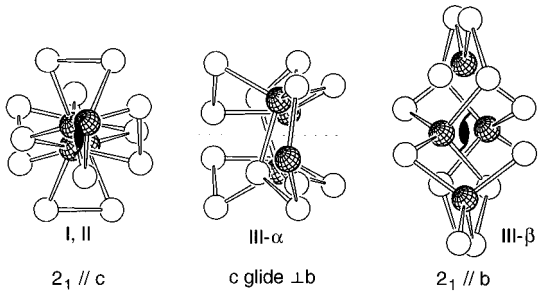

Figure 4. Views along the chain of $^1_\infty(In_2Te_6)^{2-}]$ for **I, III-α**, and **III-*β***. The screw axis (2_1) in **I**, **II**, and **III-*β*** and the glide plane (*c*-glide) in **III-α** are indicated in the figure. The cross-hatched circles are In atoms and the open circles Te.

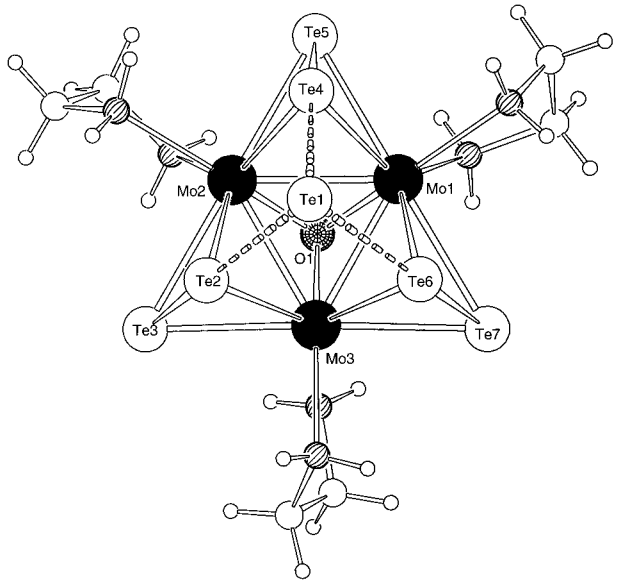

Figure 5. View of the cation $[Mo_3(en)_3(\mu_2\text{-}Te_2)_3(\mu_3\text{-}Te)(\mu_3\text{-}O)]^{2+}$ in **III-α** and **III-*β***. The solid circles are Mo, the shaded circles N, the cross-hatched circle O, and the open circles Te.

bridging S, Se, or O atom. However, the Mo_3 cluster cation reported here is the first example for Q = Te and Q′ = O. The only other Mo/Te cluster reported in the literature is $[Mo_3(CN)_6(\mu_2\text{-}Te_2)_3(\mu_3\text{-}Te)]^{2-}$ (Q, Q′ = Te).[23]

The $Mo_3(\mu_2\text{-}Q_2)_3$ part of the core region of **III-α** and **-*β*** can be described as a triangulo- Mo_3 with three edge-bridging ditelluride ligands, or as a triplet of Mo corner sharing Mo_2Te_2 tetrahedra. The bridging Te_2 dimers are elongated (2.82(4) and 2.80(2)Å for **III-α** and **-*β***) with respect to the typical covalent bond observed in the chains (Te−Te(av) = 2.755(8) Å). The tetrahedral subunits in **III-α** and **-*β*** have a Mo−Mo bond (2.719−2.733 Å) and a geometry consistent with their sulfide and selenide structures and with the three examples of $MoMTe_2$ tetrahedra (M = Fe, Te) found in the Cambridge Structrural Data system (CSD).[24] In either case, the addition of a capping O atom at one face (1.29 Å from the Mo_3 plane) tilts the ditellurides toward the opposite face to the extent that one Te atom is approximately in the Mo_3 face (see Te3, Te5, and Te7 in Figure 5). The same motif is found in $[Mo_3(\mu_2\text{-}S_2)_3(\mu_3\text{-}Q')]^{4+}$ or $[Mo_3(\mu_2\text{-}Se_2)_3(\mu_3\text{-}Q')]^{4+}$ species in which Q′ is an O, S, or Se atom at the Mo_3 face capping position, which is also the case in $[Mo_3(\mu_2\text{-}Te_2)_3(\mu_3\text{-}T)]^{4+}$ of $[Mo_3(CN)_6(\mu_2\text{-}Te_2)_3(\mu_3\text{-}Te)]^{2-}$. This arrangement in **III-α** and **-*β*** allows the three apical Te atoms (Te2, Te4, and Te6 in Figure 5) to bond to a seventh Te atom, yielding a Te_3 face capping Te atom (Te1 in Figure 5) that is approximately 2.26 Å from the Te_3 plane. The result is a three-tiered pyramid shape for the cation core and a cubic unit for Mo_3Te_3TeO (see the three Mo and O atoms and Te1, Te2, Te4, and Te6 in Figure 5). The three terminal en ligands complete the valences of the Mo atoms, with the result being $[Mo_3(en)_3(\mu_2\text{-}Te_2)_3(\mu_3\text{-}Te)(\mu_3\text{-}O)]^{2+}$. The bonding interactions between Te1 at the capping position (Te_{ca}) and the three apical Te atoms (Te_{ap}) are rather strong, giving rise to an interatomic distance of 3.03(4) Å (av) for the α phase and 3.06(6) Å (av) for the *β* phase. These are certainly longer than a typical Te−Te covalent bond distance (2.72−2.75 Å) but considerably shorter than a van der Waals distance (4.12 Å). In other triangulo−trimolybdenum(IV) compounds with bridging diselenides, similar but weaker intermolecular bonding interactions have been observed between the three apical atoms, Se_{ap}, and the face capping one (usually from a neighboring cluster unit), Se_{ca}. In fact, recent studies on the molybdenum polyselenide compounds containing the $[Mo_3Se_7]^{4+}$ cluster core have shown that there is always a tendency of this cluster to bind to a negatively charged Se_{ca} via Se_{ap} atoms.[22] A striking inverse correlation between the Se_{ap}−Se_{ca} and doubly-bridging Se−Se bond distances have been recognized and rationalized. About the Te−Te bond correlation, we have noticed the increase in the bond length for the doubly bridging $(Te_2)^{2-}$ (av 2.81Å) compared to the Te−Te covalent bonds, such as those of the $(In_2Te_6)^{2-}$ chains and of other η^2-Te_2 complexes.[25] In $[Mo_3(CN)_6(\mu_2\text{-}Te_2)_3(\mu_3\text{-}Te)]^{2-}$, where the capping position is occupied by an iodine anion, the distance between the iodine and the apical Te atom (Te_{ap}) is significantly longer, 3.576 Å, and the doubly-bridging Te_2 distance is comparable to those of other μ_2-Te_2 bonds, 2.688(2) Å.[25] The cation in the crystal structure of **III-α** differs from that of **III-*β*** by only minor dihedral variations within the en ligands. The O atom of the cation in either the α or *β* phase of **III** is apparently face capping, but it is equally possible that this site is an average of three partially occupied sites (that sum to 1.0) for O atoms that complete the three Mo_2Te_2 tetrahedra. The structure refinement yields an O atom of unit occupancy but with large displacement parameters in the direction parallel to the Mo_3 plane. The X-ray data obtained here cannot distinguish between these two cases for either **III-α** or **III-*β***.

The interatomic distances between the nearest-neighbor transition metals in the complex cations are 8.06 (**III-α**), 8.21 (**I**, **II**), and 8.23 Å (**III-*β***), respectively. For both **III-α** and **III-*β***, unpaired electrons are likely to exist for a d^2 configuration of (IV), in which cases paramagnetic behavior may be expected

(23) Fedin, V. P.; Imoto H.; Saito, T.; McFarlane, W.; Sykes, A. G. *Inorg. Chem.* **1995**, *34*, 5097.

(24) Bogan, L. E., Jr.; Rauchfuss, T. B.; Rheingold A. L. *Inorg. Chem.* **198**5, *24*, 3720. Seigneurin, A.; Makani, T.; Jones, D. J.; Roziere J. *J. Chem. Soc., Dalton Trans.* **1987**, 2111.

(25) Maxwell, L. R.; Mosley, V. M. *Phys. Rev.* **1940**, *57*, 21.

for these compounds. The divalent Fe(II) in **I** is likely to be high-spin with unpaired electrons since the Fe−N distances agree with the known Fe(II) amine complexes (2.21 Å).[18] However, further experimental evidence is needed to confirm this assumption.

Summary

While continued efforts are being made for crystal growth of new metal tellurides, we have recently synthesized a new group of indium tellurium compounds via low-temperature routes. All have been obtained from solvothermal reactions at 170−180 °C. Structural analyses on these phases have revealed a number of interesting and unique features. The one-dimensional anionic chain formed by fused five-member rings of In_2Te_3 represents a new structural motif for indium chalcogenide compounds. The Mo_3 polytelluride cluster found in α- and β-$[Mo_3(en)_3(\mu_2\text{-}Te_2)_3(\mu_3\text{-}Te)(\mu_3\text{-}O)]In_2Te_6$ is interesting for the novelty in both its structure and bonding.

Acknowledgment. Financial support from the National Science Foundation (Grants DMR-9310431 and DMR-9553066) is greatly appreciated. J.L. is also grateful to the Camille and Henry Dreyfus Foundation for a Henry Dreyfus Teacher−Scholar Award.

Supporting Information Available: Summary of crystal data, atomic positional parameters, complete list of interatomic distances and angles and torsion angles, anisotropic thermal parameters (Table S1-S24) and plots of anion chains of **I**, **II**, **III-α** and **III-*β***, showing 50% thermal vibration ellipsoids (38 pages). Ordering information is given on any current masthead page.

IC960751V